Asynchronous Common-Stream for Rate-Splitting: A Two-User MISO Analysis

Hossein Maleki and Hamid Jafarkhani

***Abstract*—The common stream in rate-splitting multiple access is decoded while private streams are treated as interference. We study a simple waveform modification for the two-user multiple-input single-output downlink where both private streams are synchronized, while the common stream is delayed. The intentional offset reduces the private interference seen by the common decoder. Ideal waveform cancellation leaves the private rates unchanged. We derive an achievable sum rate gain bound for this system. An exact high-SNR analysis characterizes the optimal power split and shows that the offset lowers the channel-correlation threshold for common-stream activation, with the gain approaching the upper bound for nearly aligned channels.**

I. Introduction

Rate-splitting (RS) manages interference by dividing user messages into common and private parts. The common parts are encoded into one stream decoded by all users, followed by successive interference cancellation (SIC) and private decoding [1]–[4]. For a two-user multiple-input single-output (MISO) broadcast channel, fixed zero-forcing (ZF) private beams provide an insightful analysis for channel strength, channel alignment, and the common/private power split [3].

Asynchronous multiple access has a long information-theoretic history [5]. Later work applied timing offsets to interference cancellation and uplink non-orthogonal multiple access (NOMA) [6]–[10], multiple-input multiple-output (MIMO) reception [11], downlink NOMA [12], virtual MIMO [13], and transmit beamforming [14]. The study in [14] shows that fractional timing reduces sampled interference variance according to pulse excess bandwidth and the reduction vanishes at zero roll-off.

These observations motivate an important question: *can a timing offset help RS even when ZF already removes interference between private streams?* In this paper, we answer this question affirmatively by intentionally adding time shifts to the common stream.. Our contribution also includes a receiver-specific analysis of this timing arrangement for general channel strengths. We show that the common-rate bound improves without changing the private rates, and bound the gain by a pulse-dependent constant, which we show is asymptotically tight at high signal-to-noise ratio (SNR). We provide a closed-form high-SNR limit for the gain and the exact channel-correlation threshold above which the common stream is worth using. To isolate and quantify the benefit of timing asynchrony, we adopt the tractable fixed spatial beam directions of [3] and optimize power allocation and timing-dependent common beam within this family. This focused formulation makes the asynchronous gain analytically transparent.

The authors are with the University of California Irvine, Irvine, CA 92697 USA. This work was supported in part by the NSF Award CCF-2328075.

II. Signal Model and Receiver

A. Asynchronous transmission

Consider a transmitter with $M \geq 2$ antennas and two single-antenna users. The flat-fading channel to User k is $\boldsymbol{h}_k \in \mathbb{C}^M$. The channel state information and timing are perfectly known by the transmitter and the receiver. Let $p(t)$ be a unit-energy pulse with symbol period T and autocorrelation

$$q(t) = \int_{-\infty}^{+\infty} p(u)p^*(u-t)\mathrm{d}u, \qquad q(nT) = \delta_n, \tag{1}$$

where δ_n equals one only for $n = 0$. Independent unit-variance Gaussian symbols form streams $s_c[n], s_1[n], s_2[n]$. The frame consists of N symbols. The transmit waveform is

$$\begin{aligned} \boldsymbol{x}(t) = \boldsymbol{w}_c \sum_{n=1}^{N} s_c[n]p(t - nT - \tau T) \\ + \sum_{j=1}^{2} \boldsymbol{w}_j \sum_{n=1}^{N} s_j[n]p(t - nT), \end{aligned} \tag{2}$$

with $0 \leq \tau < 1$. The beamformers are $\boldsymbol{w}_1$, $\boldsymbol{w}_2$, and $\boldsymbol{w}_c$ with $\sum_{j\in\{c,1,2\}} \|\boldsymbol{w}_j\|^2 \leq P$. Here, P is the average energy per symbol interval. The received waveform is $y_k(t) = \boldsymbol{h}_k^{\mathsf{H}}\boldsymbol{x}(t) + n_k(t)$. Noise is a complex additive white Gaussian $\mathcal{CN}(0, 1)$. Synchronous RS corresponds to $\tau = 0$. The analysis uses long blocks, so the extra τT of frame duration is negligible.

B. Two sampling phases and waveform cancellation

For common decoding, User k samples the matched-filter output at $nT + \tau T$, $n = 1, \ldots, N$. With $a_{kj} = \boldsymbol{h}_k^{\mathsf{H}}\boldsymbol{w}_j$, the observation is

$$\begin{aligned} y_{c,k}[n] = a_{kc}s_c[n] + z_{c,k}[n] \\ + \sum_{j=1}^{2} a_{kj} \sum_{m=1}^{N} q((n - m + \tau)T)s_j[m], \end{aligned} \tag{3}$$

where $z_{c,k}[n]$ denotes the matched-filtered noise sampled at $nT + \tau T$. For a finite block, we define

$$\eta_N(n, \tau) = \sum_{m=1}^{N} |q((n - m + \tau)T)|^2. \tag{4}$$

Let $\eta(\tau) \triangleq \sum_{\ell\in\mathbb{Z}} |q((\ell+\tau)T)|^2$. Except for the edges, $\eta_N(n,\tau)$ approaches $\eta(\tau)$ as N grows. The long-block private-interference variance is therefore $\eta(\tau)\sum_j |a_{kj}|^2$. For an ideal root-raised-cosine (RRC) pulse of roll-off β, we have [14]

$$\eta(\tau) = 1 - \frac{\beta}{4} + \frac{\beta}{4}\cos(2\pi\tau), \quad \eta(1/2) = 1 - \frac{\beta}{2}. \tag{5}$$

After decoding the common codeword, the receiver reconstructs its entire delayed waveform and subtracts it. Sampling the result at nT, $n = 1, \ldots, N$, results in

$$y_{p,k}[n] = a_{kk}s_k[n] + a_{kj}s_j[n] + z_{p,k}[n], \quad j \neq k. \tag{6}$$

III. Achievable Rates and Timing Gain

Based on the previous discussion, the achievable rate for the common stream is

$$R_{c,k}(\eta) = \log_2\left(1 + \frac{|a_{kc}|^2}{1 + \eta\sum_{j=1}^{2}|a_{kj}|^2}\right). \tag{7}$$

Under ideal SIC, the private rate is

$$R_{p,k} = \log_2\left(1 + \frac{|a_{kk}|^2}{1 + |a_{kj}|^2}\right), \quad j \neq k. \tag{8}$$

The common codeword must be decodable at both users. Hence, $R_c = \min_k R_{c,k}$ and

$$R_{\mathrm{sum}}(\eta) = R_c(\eta) + R_{p,1} + R_{p,2}. \tag{9}$$

Note that the common rate is counted once and its portions may be divided between user messages without changing (9).

Proposition 1. *For fixed spatial precoders and power allocation, and ideal SIC, the sum-rate improvement satisfies*

$$0 \leq R_{\mathrm{sum}}(\eta) - R_{\mathrm{sum}}(1) \leq \log_2\left(\frac{1}{\eta}\right). \tag{10}$$

The same bound holds when both schemes are optimized over the same feasible set of precoders and power allocations.

Proof. The private rates are independent of η. For User k, let $S_k = |a_{kc}|^2$ and $I_k = \sum_{j=1}^{2}|a_{kj}|^2$. Since $0 < \eta \leq 1$, the common rate is nondecreasing as η decreases. Moreover,

$$\frac{1 + S_k/(1+\eta I_k)}{1 + S_k/(1+I_k)} = \frac{1 + \eta I_k + S_k}{1 + I_k + S_k}\,\frac{1 + I_k}{1 + \eta I_k} \leq \frac{1}{\eta}. \tag{11}$$

Taking logarithms and then the minimum over the two users proves (10). Since the inequality holds pointwise, maximizing both schemes over the same feasible set preserves the bound. □

For a fixed design with positive common signal and private interference at both users, $\eta < 1$ strictly increases the sum-rate. Equality occurs with no common stream, no private interference, or $\beta = 0$. Half-symbol timing is optimal because (7) decreases with η and (5) is minimized at $\tau = 1/2$.

IV. Precoder and Power Design

Section III evaluated the rates of arbitrary precoders. To compare a synchronous system with a system with common-offset, and to isolate what the timing offset does, we also propose a concrete, low-complexity design. It follows the two-user construction of [3]: the private directions use ZF, the private powers are allocated by water filling, the common direction is calculated based on a max-min beamforming, and a single scalar, the fraction t of the total power given to the private streams, is searched. Joint optimization of all precoders as in [15] is not attempted, and the main focus is on showing the power of asynchrony.

The synchronous and the common-offset designs differ in exactly one place: the constant η that multiplies the private interference in the common decoder's denominator in (7). The ZF directions, the water-filled powers and the private rates are the same for both schemes at every t. The offset acts only through the common decoder, and it therefore changes the common beam and the best value of t.

A. Channel parametrization and ZF private beams

Let $\boldsymbol{h}_k = \sqrt{g_k}\,\bar{\boldsymbol{h}}_k$ with $g_k = \|\boldsymbol{h}_k\|^2$ and $\|\bar{\boldsymbol{h}}_k\| = 1$, and label the users so that $g_1 \geq g_2$. The two quantities that matter are the strength disparity g_2/g_1 and the channel-direction quantity

$$\rho = 1 - |\bar{\boldsymbol{h}}_1^{\mathsf{H}}\bar{\boldsymbol{h}}_2|^2 \in [0, 1]. \tag{12}$$

Here, $\rho = 0$ means collinear channels, where spatial separation is impossible, and $\rho = 1$ means orthogonal channels. Also, let the normalized channel correlation be $c \triangleq \left|\bar{\boldsymbol{h}}_1^{\mathsf{H}}\bar{\boldsymbol{h}}_2\right|$, such that $\rho = 1 - c^2$. We assume $\rho > 0$ since ZF is singular for $\rho = 0$, and the design reduces to common-only transmission ($t = 0$).

The ZF direction of User k is the unit-norm transmit direction that carries its private stream without leaking into the channel of other user. It is obtained by projecting $\bar{\boldsymbol{h}}_k$ onto the null space of $\bar{\boldsymbol{h}}_j$ and normalizing. That is,

$$\boldsymbol{f}_k = \frac{(\boldsymbol{I} - \bar{\boldsymbol{h}}_j\bar{\boldsymbol{h}}_j^{\mathsf{H}})\bar{\boldsymbol{h}}_k}{\sqrt{\rho}}, \quad j \neq k, \tag{13}$$

where the denominator normalizes $\|\boldsymbol{f}_k\| = 1$ because $\|(\boldsymbol{I} - \bar{\boldsymbol{h}}_j\bar{\boldsymbol{h}}_j^{\mathsf{H}})\bar{\boldsymbol{h}}_k\|^2 = 1 - |\bar{\boldsymbol{h}}_j^{\mathsf{H}}\bar{\boldsymbol{h}}_k|^2 = \rho$. By construction, we have $\boldsymbol{h}_j^{\mathsf{H}}\boldsymbol{f}_k = 0$ and $|\boldsymbol{h}_k^{\mathsf{H}}\boldsymbol{f}_k|^2 = g_k\rho$. With $\boldsymbol{w}_k = \sqrt{P_k}\,\boldsymbol{f}_k$, the coefficients of Sec. II become $a_{kj} = 0$ for $j \neq k$ and $|a_{kk}|^2 = g_k\rho P_k$. Substituting into (8) gives

$$R_{p,k} = \log_2(1 + g_k\rho P_k). \tag{14}$$

In addition, note that the private interference that reaches the common decoder of User k is only its *own* private stream, because ZF has already nulled the other one. Its power is $g_k\rho P_k$, so the common decoder sees the denominator

$$d_{k,\eta} = 1 + \eta\, g_k\rho P_k. \tag{15}$$

This denominator is the quantity that the timing offset can still reduce even though ZF removes inter-user private interference.

B. Private powers by water filling

Let $P = P_c + P_1 + P_2$, with $P_c = (1-t)P$ for the common stream and $P_1 + P_2 = tP$ for the private streams, $t \in [0,1]$. For a given t, the private powers maximize the private sum rate $\sum_k \log_2(1 + g_k \rho P_k)$, which is the classic water-filling problem with channel gains $g_k \rho$:

$$P_k = \Big[\nu - \frac{1}{g_k \rho}\Big]^+, \qquad P_1 + P_2 = tP, \tag{16}$$

where $[x]^+ = \max(x, 0)$ and ν is the water level. Define the disparity term

$$\Gamma = \frac{1}{\rho}\Big(\frac{1}{g_2} - \frac{1}{g_1}\Big) \geq 0. \tag{17}$$

Solving (16) gives two regimes:

$$(P_1, P_2) = \begin{cases} (tP,\, 0), & tP \leq \Gamma, \\ \big(\frac{tP+\Gamma}{2},\, \frac{tP-\Gamma}{2}\big), & tP > \Gamma, \end{cases} \tag{18}$$

with water level $\nu = tP/2 + (g_1^{-1} + g_2^{-1})/(2\rho)$ in the second regime. The first regime carries one private stream (the NOMA/orthogonal multiple access (OMA) modes, or multicast at $t = 0$), and the second carries two (the RS/space-division multiple access (SDMA) modes).

C. Common beam under a timing offset

User k decodes the common stream with SINR $P_c |\boldsymbol{h}_k^{\mathsf{H}} \boldsymbol{f}|^2 / d_{k,\eta}$ for a common beamformer $\boldsymbol{f}$. Both users must decode the codeword, so the common rate is set by the worst case. It is convenient to absorb the denominator into the channel,

$$\widetilde{\boldsymbol{h}}_{k,\eta} = \frac{\boldsymbol{h}_k}{\sqrt{d_{k,\eta}}}, \qquad \boldsymbol{f}_{c,\eta} = \arg\max_{\|\boldsymbol{f}\|=1} \min_{k=1,2} |\widetilde{\boldsymbol{h}}_{k,\eta}^{\mathsf{H}} \boldsymbol{f}|^2, \tag{19}$$

and to denote the resulting common gain by $G_c(t, \eta) = \min_k |\widetilde{\boldsymbol{h}}_{k,\eta}^{\mathsf{H}} \boldsymbol{f}_{c,\eta}|^2$, so that $R_c = \log_2(1 + P_c G_c)$. Note that $d_{k,\eta}$ depends on t through P_k and on the timing through η.

Problem (19) has a closed-form solution [3]. Let $\alpha_{ij} = \widetilde{\boldsymbol{h}}_{i,\eta}^{\mathsf{H}} \widetilde{\boldsymbol{h}}_{j,\eta}$ and $D = \alpha_{11} + \alpha_{22} - 2|\alpha_{12}|$. If both users are limiting (when both constraints are active), the optimal direction is

$$\begin{aligned} &\boldsymbol{f}_{c,\eta} = \lambda^{-1/2}\big(\mu_1 \widetilde{\boldsymbol{h}}_{1,\eta} + \mu_2 e^{-\mathrm{j}\angle \alpha_{12}} \widetilde{\boldsymbol{h}}_{2,\eta}\big), \\ &\begin{bmatrix} \mu_1 \\ \mu_2 \end{bmatrix} = \frac{1}{D} \begin{bmatrix} \alpha_{22} - |\alpha_{12}| \\ \alpha_{11} - |\alpha_{12}| \end{bmatrix}, \qquad \lambda = \frac{\alpha_{11}\alpha_{22} - |\alpha_{12}|^2}{D}. \end{aligned} \tag{20}$$

The phase factor $e^{-\mathrm{j}\angle \alpha_{12}}$ aligns the two effective channels before they are combined, and λ normalizes $\|\boldsymbol{f}_{c,\eta}\| = 1$. Then, both users obtain the same gain, $G_c = \lambda$. For $\eta = 1$, (19) is exactly the construction of [3]. For $\eta < 1$ we have $d_{k,\eta} = (1-\eta) + \eta\, d_{k,1}$. Therefore, reusing the synchronous beam would be suboptimal.

D. Sum rate and the scalar search

With the private allocation (18) and common power $P_c = (1-t)P$, the sum rate of the design for a given t is

$$F_\eta(t) = \sum_{k=1}^{2} \log_2(1 + g_k \rho P_k) + \log_2\Big(1 + P_c\, G_c(t, \eta)\Big). \tag{21}$$

The endpoints are the usual special cases. At $t = 0$, all power is common (multicast), i.e., $P_k = 0$, so $d_{k,\eta} = 1$, and the timing offset does not have an effect. At $t = 1$, there is no common stream (ZF-SDMA, or OMA when $P_2 = 0$), so the offset again has no effect. The gain from timing can appear only for $0 < t < 1$, where there is both a common stream and private interference. Although the water-filled powers are piecewise affine in t, the resulting sum-rate objective is not piecewise linear. It contains logarithmic private-rate terms and a timing-dependent max–min common gain whose active solution can change with t. Therefore, we do not assume that the function is concave or unimodal (i.e., has a single peak). Instead, we maximize it using a fine grid search over $[0, 1]$, followed by local refinement around the best grid point.

The complete procedure for given $(\boldsymbol{h}_1, \boldsymbol{h}_2, P, \eta)$ is:

1) Compute g_k, $\bar{\boldsymbol{h}}_k$, ρ (12) and the ZF directions $\boldsymbol{f}_k$ (13).
2) For each candidate t, set $P_c = (1-t)P$ and the private powers P_k by (18).
3) Form $d_{k,\eta}$ (15) and $\widetilde{\boldsymbol{h}}_{k,\eta}$, and obtain $\boldsymbol{f}_{c,\eta}$ and G_c from (19)–(20).
4) Evaluate $F_\eta(t)$ in (21), and select the t that maximizes it.

E. High-SNR limit

Define $\kappa_\eta = 1 - \eta(1-c)$ and let

$$m(\kappa) = \max_{t \in [0,1]} t(1 - \kappa t) = \begin{cases} 1 - \kappa, & \kappa < \frac{1}{2}, \\ \dfrac{1}{4\kappa}, & \kappa \geq \frac{1}{2}, \end{cases} \tag{22}$$

where the maximum is attained at $t = \min\{1, 1/(2\kappa)\}$. Let $R_\eta^\star = \max_{t\in[0,1]} F_\eta(t)$ be the optimized rate (21) based on the proposed design. Before stating the main result, we need the following lemma:

Lemma 1. *For $\boldsymbol{a}, \boldsymbol{b} \in \mathbb{C}^M$, define*

$$v(\boldsymbol{a}, \boldsymbol{b}) \triangleq \max_{\|\boldsymbol{f}\|=1} \min\Big\{|\boldsymbol{a}^{\mathsf{H}} \boldsymbol{f}|^2, |\boldsymbol{b}^{\mathsf{H}} \boldsymbol{f}|^2\Big\}. \tag{23}$$

The following properties hold:

(i) *For every $s > 0$,*

$$v(s\boldsymbol{a}, s\boldsymbol{b}) = s^2 v(\boldsymbol{a}, \boldsymbol{b}). \tag{24}$$

(ii) *The function v is locally Lipschitz continuous in $(\boldsymbol{a}, \boldsymbol{b})$.*

(iii) *If $\|\boldsymbol{a}\| = \|\boldsymbol{b}\| = \sqrt{\alpha}$, with $\alpha > 0$, then*

$$v(\boldsymbol{a}, \boldsymbol{b}) = \frac{\alpha + |\boldsymbol{a}^{\mathsf{H}} \boldsymbol{b}|}{2}. \tag{25}$$

Proof. Property (i) follows immediately from $|(s\boldsymbol{a})^{\mathsf{H}} \boldsymbol{f}|^2 = s^2 |\boldsymbol{a}^{\mathsf{H}} \boldsymbol{f}|^2$.

To prove property (ii), consider two channel pairs $(\boldsymbol{a}, \boldsymbol{b})$ and $(\boldsymbol{a}', \boldsymbol{b}')$. For every unit-norm $\boldsymbol{f}$,

$$\left| |\boldsymbol{a}^{\mathsf{H}} \boldsymbol{f}|^2 - |\boldsymbol{a}'^{\mathsf{H}} \boldsymbol{f}|^2 \right| \leq (\|\boldsymbol{a}\| + \|\boldsymbol{a}'\|)\|\boldsymbol{a} - \boldsymbol{a}'\|. \tag{26}$$

The corresponding bound holds for $\boldsymbol{b}$ and $\boldsymbol{b}'$. Moreover,

$$\left| \min_i x_i - \min_i y_i \right| \leq \max_i |x_i - y_i|. \tag{27}$$

Taking the maximum over $\|\boldsymbol{f}\| = 1$ results in

$$\begin{aligned} &|v(\boldsymbol{a}, \boldsymbol{b}) - v(\boldsymbol{a}', \boldsymbol{b}')| \\ &\quad \leq \max \Big\{ (\|\boldsymbol{a}\| + \|\boldsymbol{a}'\|)\|\boldsymbol{a} - \boldsymbol{a}'\|, \\ &\qquad\qquad (\|\boldsymbol{b}\| + \|\boldsymbol{b}'\|)\|\boldsymbol{b} - \boldsymbol{b}'\| \Big\}. \end{aligned} \tag{28}$$

On every bounded set, the norm factors on the right-hand side are bounded, proving local Lipschitz continuity.

For property (iii), the smaller of two nonnegative quantities cannot exceed their average. Hence, for every unit-norm $\boldsymbol{f}$,

$$\begin{aligned} \min \left\{ |\boldsymbol{a}^{\mathsf{H}} \boldsymbol{f}|^2, |\boldsymbol{b}^{\mathsf{H}} \boldsymbol{f}|^2 \right\} &\leq \frac{1}{2} \boldsymbol{f}^{\mathsf{H}} (\boldsymbol{a}\boldsymbol{a}^{\mathsf{H}} + \boldsymbol{b}\boldsymbol{b}^{\mathsf{H}}) \boldsymbol{f} \\ &\leq \frac{1}{2} \lambda_{\max}(\boldsymbol{a}\boldsymbol{a}^{\mathsf{H}} + \boldsymbol{b}\boldsymbol{b}^{\mathsf{H}}). \end{aligned} \tag{29}$$

Because $\|\boldsymbol{a}\|^2 = \|\boldsymbol{b}\|^2 = \alpha$, the two nonzero eigenvalues of $\boldsymbol{a}\boldsymbol{a}^{\mathsf{H}} + \boldsymbol{b}\boldsymbol{b}^{\mathsf{H}}$ are $\alpha \pm |\boldsymbol{a}^{\mathsf{H}} \boldsymbol{b}|$. Therefore,

$$v(\boldsymbol{a}, \boldsymbol{b}) \leq \frac{\alpha + |\boldsymbol{a}^{\mathsf{H}} \boldsymbol{b}|}{2}. \tag{30}$$

Let $\theta = -\angle(\boldsymbol{a}^{\mathsf{H}} \boldsymbol{b})$ and choose $\boldsymbol{f} = \frac{\boldsymbol{a} + e^{\mathrm{j}\theta} \boldsymbol{b}}{\|\boldsymbol{a} + e^{\mathrm{j}\theta} \boldsymbol{b}\|}$. This phase choice gives $\boldsymbol{a}^{\mathsf{H}}(e^{\mathrm{j}\theta} \boldsymbol{b}) = |\boldsymbol{a}^{\mathsf{H}} \boldsymbol{b}|$. Direct substitution then yields

$$|\boldsymbol{a}^{\mathsf{H}} \boldsymbol{f}|^2 = |\boldsymbol{b}^{\mathsf{H}} \boldsymbol{f}|^2 = \frac{\alpha + |\boldsymbol{a}^{\mathsf{H}} \boldsymbol{b}|}{2}. \tag{31}$$

Thus, the upper bound in (30) is attained, proving (25). $\square$

Theorem 1. *Let* $g_1 \geq g_2 > 0$, $0 \leq c < 1$ *and* $0 < \eta \leq 1$, *and let* $K = \log_2(g_1 g_2 \rho^2/4)$. *As* $P \to \infty$*:*

(a) *every maximizer* $t_\eta^\star$ *of* F_η *converges to* $t_\infty(\eta, c) = \min\{1, 1/(2\kappa_\eta)\}$*;*

(b) $R_\eta^\star = 2\log_2 P + K + \log_2 \dfrac{m(\kappa_\eta)}{\eta(1-c)} + o(1)$*;*

(c) $R_\eta^\star - R_1^\star \to Q_\infty(c, \eta) = \log_2 \dfrac{m(\kappa_\eta)}{\eta\, m(c)}$, *that is,*

$$Q_\infty(c, \eta) = \begin{cases} 0, & c \leq 1 - \dfrac{1}{2\eta}, \\ \log_2 \dfrac{1}{4\eta(1-c)\kappa_\eta}, & 1 - \dfrac{1}{2\eta} < c < \dfrac{1}{2}, \\ \log_2 \dfrac{c}{\eta\, \kappa_\eta}, & c \geq \dfrac{1}{2}. \end{cases} \tag{32}$$

The limits do not depend on g_1, g_2, *except through the additive term* K *in (b), which cancels in (c).*

Proof. Let $\bar{F}(t) = F_\eta(t) - 2\log_2 P - K$ and $\varphi_\eta(t) = t^2 + t(1-t)/(\eta(1-c)) = t(1 - \kappa_\eta t)/(\eta(1-c))$. Since $0 < \kappa_\eta < 1$, φ_η is a strictly concave quadratic with $\varphi_\eta(0) = 0$, and $\varphi_\eta > 0$ on $(0, 1]$. Its unique maximizer on $[0, 1]$ is $t_\infty = \min\{1, 1/(2\kappa_\eta)\} \geq \frac{1}{2}$, with maximum $m(\kappa_\eta)/(\eta(1-c))$. Fix $\delta \in (0, 1)$ and let $P > 2\Gamma/\delta$, so that $tP > \Gamma$ for all $t \geq \delta$ and (18) gives $P_k = (tP \pm \Gamma)/2$. Then, $1 + g_k \rho P_k = \frac{1}{2} g_k \rho t P\,(1 + O(1/(\delta P)))$ and $d_{k,\eta} = \frac{1}{2} \eta g_k \rho t P\,(1 + O(1/(\delta P)))$, uniformly in $t \in [\delta, 1]$. The effective channels are therefore $\widetilde{\boldsymbol{h}}_{k,\eta} = \bar{s}\,(1 + e_k)\bar{\boldsymbol{h}}_k$ with $\bar{s}^2 = 2/(\eta\rho t P)$ and $|e_k| = O(1/(\delta P))$. By Lemma 1, with $\|\bar{\boldsymbol{h}}_k\| = 1$ and $|\bar{\boldsymbol{h}}_1^{\mathsf{H}} \bar{\boldsymbol{h}}_2| = c$,

$$\begin{aligned} G_c &= \bar{s}^2 \Big(\tfrac{1+c}{2} + O\big(\tfrac{1}{\delta P}\big) \Big), \\ P_c G_c &= \frac{(1-t)(1+c)}{\eta \rho\, t} \big(1 + O(\tfrac{1}{\delta P})\big). \end{aligned} \tag{33}$$

Substituting into (21) yields

$$F_\eta(t) = \log_2\big(\tfrac{1}{4} g_1 g_2 \rho^2 t^2 P^2\big) + \log_2\Big(1 + \tfrac{(1-t)(1+c)}{\eta\rho t}\Big) + o(1), \tag{34}$$

that is, $\bar{F}(t) = \log_2 \varphi_\eta(t) + o(1)$ uniformly on $[\delta, 1]$.

Now, let $t \in [0, \delta]$. Since $g_1 \geq g_2$, water filling gives $P_1 \geq P_2$ and $P_1 \geq tP/2$, and $P_1 + P_2 = tP$. The common gain is at most that of User 1 alone, $G_c \leq g_1/d_{1,\eta} \leq 2/(\eta\rho t P)$, hence $P_c G_c \leq 2/(\eta\rho t)$. The private terms obey $1 + g_k \rho P_k \leq 1 + g_1 \rho t P$. If $tP \geq 1$, then

$$\bar{F}(t) \leq 2\log_2(1 + g_1\rho) + \log_2\big(t^2 + \tfrac{2t}{\eta\rho}\big) - K \leq \log_2 t + C_1, \tag{35}$$

where $C_1 = 2\log_2(1 + g_1\rho) + \log_2(1 + 2/(\eta\rho)) - K$ is independent of P and δ. If $tP < 1$, then $F_\eta(t) \leq 2\log_2(1 + g_1\rho) + \log_2(1 + g_1 P) = \log_2 P + O(1)$, so $\bar{F}(t) \to -\infty$. Hence, for large P, we have $\sup_{t \in [0,\delta]} \bar{F}(t) \leq \log_2 \delta + C_1$.

Choose $\delta < \frac{1}{2}$ with $\log_2 \delta + C_1 < \log_2 \varphi_\eta(t_\infty) - 1$. For large P, we have $\max_{[\delta,1]} \bar{F} = \log_2 \varphi_\eta(t_\infty) + o(1)$, which exceeds the bound of $t \in [0, \delta]$. So, the maximum over $[0, 1]$ lies in $[\delta, 1]$, which proves (b). Since $\bar{F} \to \log_2 \varphi_\eta$ uniformly on $[\delta, 1]$ and φ_η has the unique maximizer t_∞, every maximizer converges to t_∞, which proves (a). Applying (b) with η and with 1 (for which $\kappa_1 = c$) and subtracting, K cancels and $R_\eta^\star - R_1^\star \to \log_2 \frac{m(\kappa_\eta)}{\eta(1-c)} \frac{1-c}{m(c)} = Q_\infty(c, \eta)$. The three cases of (32) follow from (22). If $c \leq 1 - 1/(2\eta)$, then $\kappa_\eta \leq \frac{1}{2}$ and $c \leq \frac{1}{2}$, so $m(\kappa_\eta) = \eta(1-c)$ and $m(c) = 1 - c$. If $1 - 1/(2\eta) < c < \frac{1}{2}$, then $m(\kappa_\eta) = 1/(4\kappa_\eta)$ and $m(c) = 1 - c$. If $c \geq \frac{1}{2}$, then $\kappa_\eta \geq c \geq \frac{1}{2}$ and $m(c) = 1/(4c)$. $\square$

Corollary 1. *At high SNR, the optimal design uses a common stream* ($t_\infty < 1$) *if and only if* $c > 1 - 1/(2\eta)$, *for which* $t_\infty = 1/(2\kappa_\eta)$. *For a synchronous system, the threshold is* $c > 1/2$. *For the half-symbol offset with RRC pulses,* $\eta = 1 - \beta/2$ *and the threshold is* $c > (1-\beta)/(2-\beta)$, *independent of* g_1, g_2. *In terms of* $\rho = 1 - c^2$, *the boundary between RS and SDMA is a vertical line, at* $\rho = 8/9$ *for* $\beta = 0.5$ *versus* $\rho = 3/4$ *for the synchronous system.*

Proof. By Theorem 1(a), $t_\infty < 1$ if and only if $\kappa_\eta > \frac{1}{2}$, that is, $c > 1 - 1/(2\eta)$. With $\eta = 1$, this is $c > \frac{1}{2}$. Substituting $\eta = 1 - \beta/2$ gives $c > (1-\beta)/(2-\beta)$, which equals $\frac{1}{3}$ at $\beta = 0.5$. Since $\rho = 1 - c^2$ is decreasing in c, each threshold

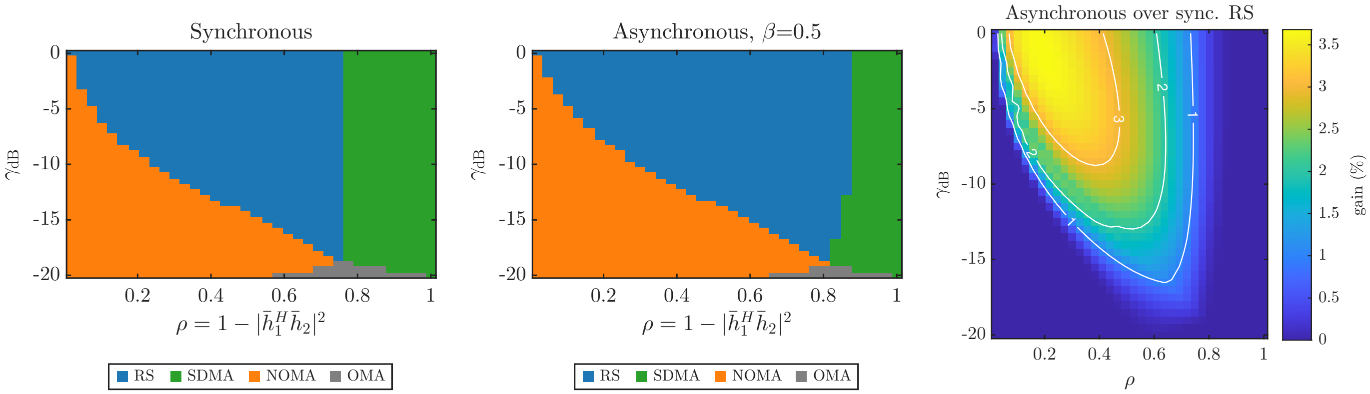

Fig. 1: Operating regions at 20 dB for synchronous and asynchronous ($\beta = 0.5$) transmission, and the resulting gain over synchronous RS.

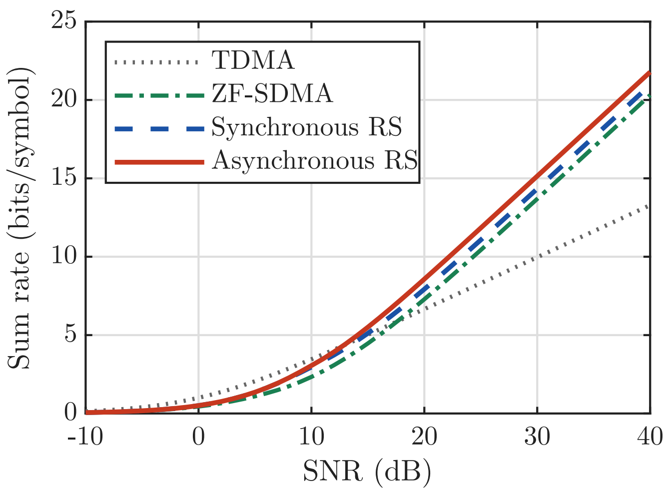

Fig. 2: Sum rates for $|\bar{\boldsymbol{h}}_1^{\mathsf{H}}\bar{\boldsymbol{h}}_2| = 0.8$, $g_1 = 1$, $g_2 = 0.4$, and $\beta = 1$.

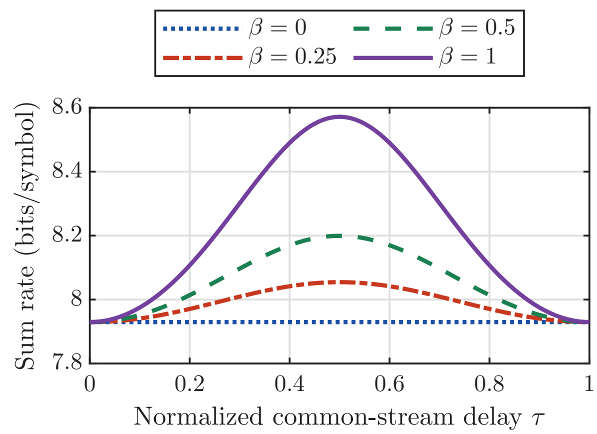

Fig. 3: Rate versus common-stream delay for $c = 0.8$.

$c > c^\star$ is equivalent to $\rho < 1 - (c^\star)^2$. At $c^\star = \frac{1}{2}$ this gives $\rho < 3/4$ for the synchronous system, and at $c^\star = \frac{1}{3}$ it gives $\rho < 1 - \frac{1}{9} = 8/9$ for $\beta = 0.5$. $\square$

V. Numerical Results

We use the canonical channels $\boldsymbol{h}_1 = [1, 0]^T$ and $\boldsymbol{h}_2 = \sqrt{0.4}[c, \sqrt{1-c^2}]^T$. Synchronous and asynchronous RS use the same ZF directions and water-filling rule, but each optimizes t and its own common direction from (19). ZF-SDMA sets $t = 1$, while single-user transmission has rate $\log_2(1 + P)$. Figures report bits per symbol interval.

Fig. 1 labels each channel pair by the special case to which the design reduces: NOMA when only one private stream is active alongside the common stream, OMA when only one private stream is active and the common stream is off, SDMA when both private streams are active and the common stream is off, and genuine RS when the common stream and both private streams are all active. The asynchronous scheme enlarges the RS region toward the SDMA side. At $\gamma_{\mathrm{dB}} = -5$ dB, the RS/SDMA boundary moves from $\rho \approx 0.75$ to $\rho \approx 0.89$, so RS becomes preferable for more channel pairs. This agrees with the high-SNR boundary of Corollary 1, which is $\rho = 0.889$ for $\beta = 0.5$ and does not depend on γ.

As shown in Fig. 2, asynchronous RS provides a bounded rate improvement over synchronous RS. At 20 dB, the gain is 0.642 bits/symbol (8.10%). At this roll-off, Proposition 1 bounds the improvement by $\log_2(1/\eta) = 1.0$ bit/symbol.

Fig. 3 shows the sum rate versus the common-stream delay τ for $c = 0.8$, confirming that $\tau = 1/2$ maximizes the rate for every roll-off β. At $\beta = 0$ timing gives no gain and at $\beta = 1$, the interference factor reaches $1/2$. Pulses with larger excess bandwidth yield greater rate gains because timing offsets suppress the sampled interference more effectively.

Fig. 4 validates Theorem 1. At 40 dB, the finite-SNR gain coincides with $Q(c, \eta)$ for $g_2 = 1$. For the much weaker $g_2 = 0.05$, the results still agree. At 20 dB, the gain remains below $Q(c, \eta)$ and collapses as $c \to 1$. Note that in the right-hand figure, the common stream activates at $c = 1/2$ for the synchronous curve and $c = 1/3$ for the asynchronous one, exactly matching the thresholds from Corollary 1.

In our analysis, we assumed ideal SIC. Suppose instead

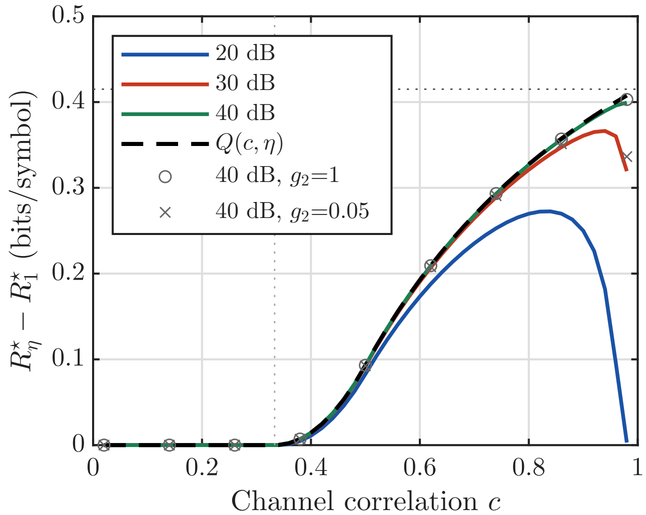

(a) Gain of the optimized asynchronous design over the synchronous design.

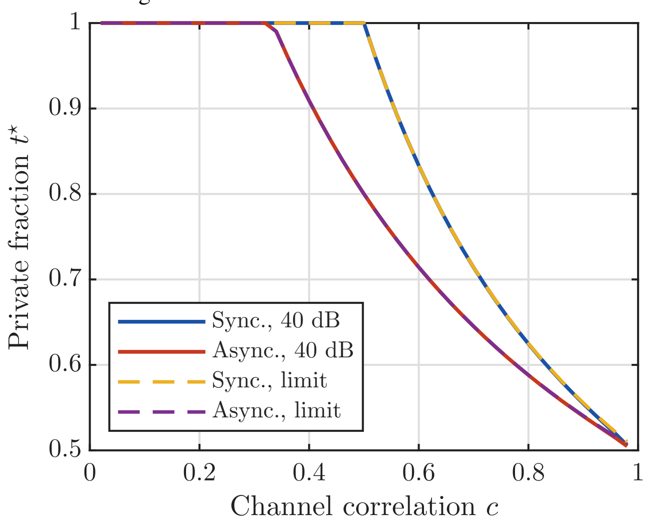

(b) Optimal private fraction at 40 dB and its asymptotic limit.

Fig. 4: Numerical verification of Theorem 1 for $\beta = 0.5$ ($\eta = 0.75$) and $g_2/g_1 = 0.4$. (a) Gain versus c at 20, 30, and 40 dB; the dashed curve is $Q(c, \eta)$, the dotted horizontal line is $\log_2(1/\eta)$, and the markers are 40 dB results for $g_2 = 1$ and $g_2 = 0.05$. (b) Optimal private fraction at 40 dB (solid) and its limit t_∞ (dashed).

that a fraction κ of the received common power remains after cancellation, as a scaled copy of the delayed common waveform. Sampled on the private grid, this residual has power $\kappa\,\eta\,|a_{kc}|^2$, so the private rate becomes

$$R_{p,k} = \log_2\Big(1 + \frac{|a_{kk}|^2}{1 + |a_{kj}|^2 + \kappa\,\eta\,|a_{kc}|^2}\Big). \qquad (36)$$

The offset therefore also shrinks the leakage of the common stream into the private decoders. Fig. 5 shows the effect. With ideal SIC, synchronous RS is 8.8% above ZF-SDMA on this channel. At $\kappa = -30$ dB, the synchronous gain is 8.0% and asynchronous RS gains 11.9% and 17.2% for $\beta = 0.5$ and 1.

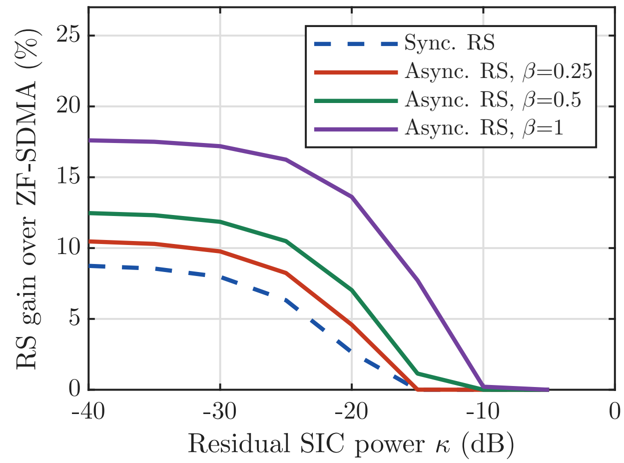

Fig. 5: Gain of RS over ZF-SDMA versus residual SIC power κ, for $c = 0.8$, $g_2/g_1 = 0.4$ and 20 dB. ZF-SDMA has no common stream and is unaffected.

At $\kappa = -20$ dB, the values are 2.6%, 7.0% and 13.6%. At $\kappa = -15$ dB, the synchronous advantage is gone (0.0%), while asynchronous RS still gains 1.1% and 7.7%. Thus, asynchrony extends the range of SIC quality over which RS beats SDMA.

VI. Conclusion

Delaying the common stream while keeping the private streams aligned improves the common-decoding rate bound in two-user MISO RS. The proposed construction follows the ZF and water-filling approach. We analyze the sum rate and quantify the improvement achieved by asynchronous transmission of the common message. We also provide a high-SNR analysis to gain further insight into this improvement. To isolate the benefits of asynchrony, we focus on a zero-forcing strategy, which is not globally optimal. Future work can investigate the optimal joint design, which may yield further gains.

References

[1] B. Clerckx, H. Joudeh, C. Hao, M. Dai, and B. Rassouli, “Rate splitting for MIMO wireless networks: A promising PHY-layer strategy for LTE evolution,” *IEEE Commun. Mag.*, vol. 54, no. 5, pp. 98–105, May 2016.

[2] Y. Mao, B. Clerckx, and V. O. K. Li, “Rate-splitting multiple access for downlink communication systems: Bridging, generalizing, and outperforming SDMA and NOMA,” *EURASIP J. Wireless Commun. Netw.*, vol. 2018, p. 133, 2018.

[3] B. Clerckx, Y. Mao, R. Schober, and H. V. Poor, “Rate-splitting unifying SDMA, OMA, NOMA, and multicasting in MISO broadcast channel: A simple two-user rate analysis,” *IEEE Wireless Commun. Lett.*, vol. 9, no. 3, pp. 349–353, March 2020.

[4] B. Clerckx, Y. Mao, E. A. Jorswieck, J. Yuan, D. J. Love, E. Erkip, and D. Niyato, “A primer on rate-splitting multiple access: Tutorial, myths, and frequently asked questions,” *IEEE J. Sel. Areas Commun.*, vol. 41, no. 5, pp. 1265–1308, May 2023.

[5] S. Verdú, “The capacity region of the symbol-asynchronous gaussian multiple-access channel,” *IEEE Trans. Inf. Theory*, vol. 35, no. 4, pp. 733–751, July 1989.

[6] H. Haci, H. Zhu, and J. Wang, “Performance of non-orthogonal multiple access (NOMA) with a novel asynchronous interference cancellation technique,” *IEEE Trans. Commun.*, vol. 65, no. 3, pp. 1319–1335, March 2017.

[7] X. Zou, B. He, and H. Jafarkhani, “An analysis of two-user uplink asynchronous non-orthogonal multiple access systems,” *IEEE Trans. Wireless Commun.*, vol. 18, no. 2, pp. 1404–1418, February 2019.

[8] M. Ganji, X. Zou, and H. Jafarkhani, “Asynchronous transmission for multiple access channels: Rate-region analysis and system design for uplink NOMA,” *IEEE Trans. Wireless Commun.*, vol. 20, no. 7, pp. 4364–4378, July 2021.

[9] S. Poorkasmaei and H. Jafarkhani, “Asynchronous orthogonal differential decoding for multiple access channels,” *IEEE Trans. Wireless Commun.*, vol. 14, no. 1, pp. 481–493, 2015.

[10] M. Ganji and H. Jafarkhani, “Interference mitigation using asynchronous transmission and sampling diversity,” in *Proc. IEEE Global Telecomm. Conf.*, 2016, pp. 1–6.

[11] A. Das and B. D. Rao, “MIMO systems with intentional timing offset,” *EURASIP J. Adv. Signal Process.*, vol. 2011, p. 267641, 2011.

[12] M. Ganji and H. Jafarkhani, “Time asynchronous NOMA for downlink transmission,” in *Proc. IEEE Wireless Commun. and Networking Conf.*, April 2019, pp. 1–6.

[13] H. Maleki and H. Jafarkhani, “Delay-domain single-antenna MIMO,” in *Proc. IEEE Semiannual Veh. Technol. Conf.*, 2026, pp. 1–5.

[14] M. Ganji, X. Zou, and H. Jafarkhani, “Exploiting time asynchrony in multi-user transmit beamforming,” *IEEE Trans. Wireless Commun.*, vol. 19, no. 5, pp. 3156–3169, May 2020.

[15] H. Joudeh and B. Clerckx, “Sum-rate maximization for linearly precoded downlink multiuser MISO systems with partial CSIT: A rate-splitting approach,” *IEEE Trans. Commun.*, vol. 64, no. 11, pp. 4847–4861, November 2016.